

# Weierstraß–Institut für Angewandte Analysis und Stochastik

im Forschungsverbund Berlin e.V.

Preprint

ISSN 0946 – 8633

## Impact of Gain Dispersion on the Spatio-temporal Dynamics of Multisection Lasers

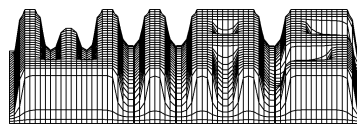
Uwe Bandelow, Mindaugas Radziunas, Jan Sieber, Matthias Wolfrum<sup>1</sup>

submitted: 13th July 2000

<sup>1</sup> all at  
Weierstrass Institute  
for Applied Analysis  
and Stochastics  
Mohrenstr. 39  
D - 10117 Berlin  
Germany  
E-Mail: bandelow, radziunas, sieber, wolfrum @wias-berlin.de

Preprint No. 597

Berlin 2000



---

2000 *Mathematics Subject Classification.* 78A60,37N20, 35B40.

*Key words and phrases.* Multi-section DFB-Lasers, traveling wave equations, high frequency self-pulsations, gain dispersion, polarization.

Edited by  
Weierstraß-Institut für Angewandte Analysis und Stochastik (WIAS)  
Mohrenstraße 39  
D — 10117 Berlin  
Germany

Fax: + 49 30 2044975  
E-Mail (X.400): c=de;a=d400-gw;p=WIAS-BERLIN;s=preprint  
E-Mail (Internet): preprint@wias-berlin.de  
World Wide Web: <http://www.wias-berlin.de/>

## Abstract

We present a refined model for multi-section lasers, introducing an additional equation for material polarization in the well known travelling wave model. We investigate the polarization-induced changes in the spectral properties of the optical waveguide. Finally, we show the relevance of this model for a more realistic simulation of complicated dynamical behaviour of multi-section Distributed Feedback (DFB)-Lasers, such as fast self-pulsations, multi-stability, and hysteresis effects due to mode competition.

## 1 Introduction

Multi-section DFB (Distributed Feedback) Lasers exhibit a broad range of complicated spatio-temporal dynamics. Self-pulsations, multi-stability, hysteresis, and even chaotic behavior can be observed in both experiments and numerical simulations [2],[11]. Especially high frequency self-pulsations and their capability of locking onto external signals can be used for clock-recovery in all-optical signal regeneration [10]. However, the onset of these self-pulsations is accompanied with a complicated, often hysteretic switching behaviour between different operating states, depending strongly on the operating conditions.

This is mathematically described by the long-time behaviour and the bifurcations of a nonlinear system of model equations including different time scales. Due to their nonlinearity, these effects can be very sensitive to changes in the parameters and the structure of the model. Indeed, even though the nonlinear material gain dispersion is a comparatively small effect, it turned out that its influence on mode competition can cause drastic changes in the dynamical long-time behaviour. However, the design of self-pulsating laser devices for optical communication applications requires a highly accurate simulation of these dynamical effects to obtain their dependence on the set of design and control parameters.

In this paper we discuss a model which extends the well-known traveling wave model [7, 15] with additional polarization equations. This extended model reflects spectral selectivity due to the geometry of the device (waveguide dispersion) as well as dispersion due to material properties. We first discuss the theoretical background and fundamental assumptions for this model. Then we show that our formulation of the nonlinear gain dispersion allows to extend the results from [12, 13] about the spectral properties of the resonator. Using these results, further analytic investigations on finite dimensional approximations, bifurcation theory and locking behaviour (see

[2, 16, 3] for the travelling wave equations) may be performed for the extended model in the same way.

Finally we demonstrate the importance of the extended model for accurate simulation of high frequency self pulsating devices.

## 2 Traveling wave equations including polarization

A standard model for studying the longitudinal behaviour of DFB-lasers are the so called traveling wave equations (TWE) (see e.g. [7, 15]). They describe the evolution of an optical field  $E(\vec{r}, t)$

$$\mathbf{E}(\vec{r}, t) = E(x, y)(\Psi^+(z, t)e^{i(\omega_0 t - \frac{\pi}{\Lambda} z)} + \Psi^-(z, t)e^{i(\omega_0 t + \frac{\pi}{\Lambda} z)})$$

along the propagation direction  $z$  in transverse single mode approximation. The evolution of the slowly varying complex amplitudes  $\Psi(z, t) = (\Psi^+(z, t), \Psi^-(z, t))$  is governed by the equations

$$-i\partial_t \Psi^\pm = \nu(\pm i\partial_z \Psi^\pm - \beta(\mathbf{N})\Psi^\pm - \kappa\Psi^\mp) \quad (1)$$

for  $0 \leq z \leq L$ ,  $t \geq 0$  and boundary conditions  $\Psi^+(0, t) = r_0\Psi^-(0, t)$ ,  $\Psi^-(L, t) = r_L\Psi^+(L, t)$ . Here,  $\nu$  is the group velocity, and the real coefficient  $\kappa$  describes an index coupling by a Bragg-corrugation in the waveguide. In our numerical calculations we included spontaneous emission in (1) by an additional small stochastic source term.

The propagation factor  $\beta$  is assumed to be piecewise constant in  $z$  and modeled as

$$\beta(N_k) = \delta_k - i\frac{\alpha_{0k}}{2} + \frac{i + \alpha_{Hk}}{2}g_k(N_k - N_k^{tr})$$

where detuning  $\delta$ , losses  $\alpha_0$ , Henry-factor  $\alpha_H$ , differential gain  $g$ , and transparency carrier density  $N^{tr}$  are constant in each section  $S_k$ . The model is completed by rate equations for the carrier densities  $\mathbf{N} = (N_1, \dots, N_s)$ , where each  $N_k$  is the density, averaged over one separately pumped section  $S_k$  of the device:

$$\frac{d}{dt}N_k = \frac{I_k}{eV_k} - \frac{N_k}{\tau_k} - \nu g_k(N_k - N_k^{tr})\langle \Phi, \Psi \rangle_k \quad (2)$$

Here,  $V_k$  is the Volume,  $\tau_k$  the spontaneous recombination lifetime, and  $I_k$  the pumping current in the  $k$ -th section, respectively. The integral

$$\langle \Phi, \Psi \rangle_k = \frac{1}{V_k} \int_{S_k} \Phi^{+*} \Psi^+ + \Phi^{-*} \Psi^- dz.$$

is the photon density in the  $k$ -th section  $S_k$  and is proportional to the optical power.

To study effects of spatial hole burning, one can also allow for spatial variation of the carriers within the sections. Nevertheless, for our purposes the piecewise constant version is sufficient. Such models have been widely used for numerical simulations,

reproducing a lot of the complicated spatio-temporal dynamical behaviour of transversely single-moded integrated devices which have a complex longitudinal structure [11]. On the other hand these equations are still simple enough to allow for analytic investigations which may give an explanation of the basic mechanisms, leading to certain nonlinear phenomena [16, 3]. It fails, however, to describe devices where the emission is determined by the dispersion of the material alone, rather than the spectral selectivity of the resonator, as for example Fabry-Perot lasers. It may fail in the same way under conditions where a more complicated resonator simultaneously supports several longitudinal modes at different wavelengths.

To overcome this problem, we introduce nonlinear gain dispersion. Such dispersion enters via the frequency dependence of the displacement  $\mathbf{D}(\omega)$ , the time derivative of which appears in the original Maxwell equations. Hence, in the frequency domain, one has to deal with an expression of the form  $\omega\mathbf{D}(\omega)$  which is modeled as

$$\omega\mathbf{D}(\omega) = \varepsilon_0 \left( \omega_0\varepsilon(\omega_0) + \frac{\partial\omega\varepsilon(\omega)}{\partial\omega}(\omega - \omega_0) \right) \mathbf{E}(\omega) + \omega_0\mathbf{P}(\omega) \quad (3)$$

in the vicinity of the reference frequency,  $\omega \approx \omega_0$ . The first term containing the linear frequency dependence has already been proposed by Landau [5] for dispersive dielectrics. Taking this term alone, the traveling wave equations (1) can be derived [14], using suitable assumptions. As proposed e.g. in [9], we fit the nonlinear polarization by a Lorentzian:

$$\mathbf{P}(\omega) = \varepsilon_0\chi(\omega)\mathbf{E}(\omega) = \varepsilon_0\frac{\Gamma G_r}{2(\omega - \Omega_r - i\Gamma)}\mathbf{E}(\omega).$$

Inverse Fourier transformation then yields a differential equation for  $\mathbf{P}(t)$ :

$$-i\frac{d}{dt}\mathbf{P}(t) = (\Omega_r + i\Gamma)\mathbf{P}(t) + \Gamma\frac{\varepsilon_0 G_r}{2}\mathbf{E}(t). \quad (4)$$

In general, the parameters  $\Gamma$ ,  $G_r$ ,  $\Omega_r$  of the Lorentzian may be space dependent. For a derivation of the corresponding traveling wave equations, see [14]. Here, it is sufficient to assume these parameters to be spatially constant in each section, and we obtain from (3) and (4)

$$\frac{2}{\varepsilon_0 G_r}\mathbf{P}(\vec{r}, t) = E(x, y) \cdot (p^+(z, t)e^{i(\omega_0 t - \frac{\pi}{\Lambda}z)} + p^-(z, t)e^{i(\omega_0 t + \frac{\pi}{\Lambda}z)}), \quad (5)$$

together with the evolution equation for the slowly varying amplitudes  $\mathbf{p}(z, t) = (p^+(z, t), p^-(z, t))$  which reads

$$-i\frac{d}{dt}p^\pm = (\Omega_r + i\Gamma)p^\pm + \Gamma\Psi^\pm. \quad (6)$$

The equations (1) and (2) have to be adapted appropriately (see [14] for details),

$$-i\partial_t\Psi^\pm = \nu \left[ (\pm i\partial_z - \beta(\mathbf{N}))\Psi^\pm - \kappa\Psi^\mp - \frac{G_r}{2}p^\pm \right] \quad (7)$$

$$\frac{d}{dt}N_k = \frac{I_k}{eV_k} - \frac{N_k}{\tau_k} - \nu(g_k(N_k - N_k^{tr}) - G_r)\langle\Psi, \Psi\rangle_k - G_r \text{Im}(\langle\Psi, \mathbf{p}\rangle_k) \quad (8)$$

where now the propagation factor is given by

$$\beta(N_k) = \delta_k - i\frac{\alpha_{0k}}{2} + \frac{i + \alpha_{Hk}}{2}g_k(N_k - N_k^{tr}) - i\frac{G_r}{2}. \quad (9)$$

We finally end up with the system of equations (6),(7),(8). Note that  $p^\pm$  in equation (6) depends only parametrically on  $z$ . As a linear ODE, it could be integrated and included as an integral convolution operator in (7). For our purposes, however, the given form is more convenient. Moreover, since we keep the non dispersive part of the gain by (9) in the electrical field equation (7), it allows for a straight-forward adiabatic elimination of the polarization, leading back to the standard TWE model.

Indeed, similar approaches where the material gain dispersion is modeled by a convolution term can be found in [1],[8]. Moreover, in [6], [7],[4] digital filtering techniques have been applied in numerical simulations to include effects of nonlinear gain dispersion, determining the filter parameters by fitting gain spectra obtained from microscopic models or experiments.

In the sequel we will give a systematic investigation of how the nonlinear gain dispersion influences the spectral properties of the field operator, compared to the standard TWE equation. Furthermore, we demonstrate by numerical simulations that due to the nonlinearity of the system, already a small amount of nonlinear gain dispersion may lead to significant changes in the dynamical behavior of a multi-section DFB-laser.

### 3 The spectrum of the optical part

An important property of semiconductor laser models is the large ratio of carrier versus photon lifetime, typically being two orders of magnitude. This ratio leads to different time scales between (8) and (6), (7). Eq. (8) governs slowly varying carrier densities, whereas (6), (7) governs the fast “optical” subsystem. The optical subsystem (6), (7) is linear in the field and polarization amplitudes and can be expressed in compact form as an operator equation

$$-i\partial_t \begin{pmatrix} \Psi \\ \mathbf{p} \end{pmatrix} = H(\mathbf{N}) \begin{pmatrix} \Psi \\ \mathbf{p} \end{pmatrix}. \quad (10)$$

The coefficients in the operator

$$H(\mathbf{N}) = \begin{pmatrix} H_0 + i\nu\frac{G_r}{2} & -\nu\frac{G_r}{2} \\ \Gamma & \Omega_r + i\Gamma \end{pmatrix} \quad (11)$$

parametrically depend on the slowly varying carrier density  $\mathbf{N}$ . Within (11)  $H_0$  is the operator on the r.h.s. of (1) without material gain dispersion, whereas all other parameters in (11) are due to material gain dispersion and cause a coupling between the optical field and the polarization. Nevertheless, the optical subsystem is still linear in these quantities and permits an expansion into a series of eigenfunctions of

$H(\mathbf{N})$  which we refer to as instantaneous (i. e.  $\mathbf{N}$ -dependent) modes. Furthermore, the operator  $H(\mathbf{N})$  is not self-adjoint and hence its eigenvalues will be complex. We interpret the real part of each eigenvalue  $\omega$  as the frequency (corresponding to the wavelength) and the imaginary part as the decay rate (corresponding to the reverse lifetime) of the corresponding mode.

Often,  $\mathbf{N}$  varies only in a small range near a threshold value. In such cases the decay rates of the instantaneous modes determine the long-time behaviour of the laser. Usually, only one or a few modes with the smallest decay rates contribute to the optical field. This allows for insightful, low-dimensional mode approximation being models. This has been done previously for the TWE (1) in [3, 16, 10], and we extend this analysis here to equation (10). In other words, we are now concerned with the spectrum of  $H$ , determined by

$$\omega \Psi = H_0 \Psi + i\nu \frac{G_r}{2} \Psi - \nu \chi(\omega) \Psi. \quad (12)$$

In particular, we will point out the differences to the spectrum of  $H_0$  (c.f. [12, 13]) that are introduced by the polarization equations.

### 3.1 Mode Spectrum of a Fabry-Perot Laser

In a Fabry-Perot laser gain dispersion is the main mechanism leading to mode selectivity. Without gain dispersion all eigenvalues

$$\omega_l = \frac{\nu}{L} \left( - \sum_{k=1}^{n_s} \beta_k L_k - \frac{i}{2} \log(r_0 r_L) - \pi l \right). \quad (13)$$

obtain the same decay rate. Here,  $L_k$  is the length of the  $k$ th section and  $n_s$  is the number of sections. As no mode selectivity at all is not realistic, we must take the gain dispersion into account. According to (12), the eigenvalues  $\omega$  solve the equations

$$\omega = \frac{\nu}{L} \left[ - \sum_{k=1}^{n_s} \left( -i \frac{G_{r,k}}{2} + \chi_k(\omega) \right) L_k \right] + \omega_l. \quad (14)$$

This formula is implicit but it can be solved for  $\omega$  by a simple iteration starting from the eigenvalues  $\omega_l$  from (13). Suggested by measurements we have used the following parameters for the polarization:

$$G_r = 40 \text{ cm}^{-1}, \quad \Omega_r = -\frac{\omega_0^2}{2\pi c} \cdot 5nm, \quad \Gamma = \frac{\omega_0^2}{2\pi c} \cdot 75nm. \quad (15)$$

For these parameters, a single iteration is sufficiently accurate. Then, we can replace  $\chi_k(\omega)$  in (14) by  $\chi_k(\omega_l)$  such that the eigenvalue sequence of the Fabry-Perot resonator directly reflects the Lorentzian fit of the gain dispersion (see the lower part of Fig.1). These eigenvalues correspond to the *optical* modes of  $H$ . Additionally, as shown in the upper part of Fig.1, the inclusion of the polarization equation induces

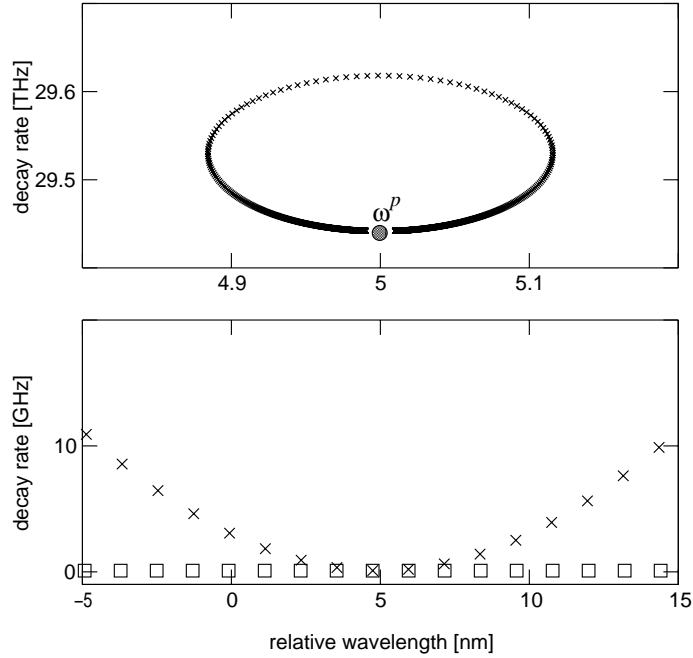


Figure 1: Modes of a single section Fabry-Perot laser at the threshold with (crosses) and without (boxes) gain dispersion taken into account. The polarization modes, shown in the upper part, accumulate at the complex relative resonance frequency (black dot). Note that the two parts of the picture have different scalings.

an infinite set of *polarization* modes for each section  $k$  with gain dispersion. Apparently, these polarization modes are strongly damped with decay rates  $\sim \Gamma_k$  and they accumulate at the point  $\omega_k^p := \Omega_{rk} + i\Gamma_k$ . Typical gain dispersion visible in Fig.1 leads to decay rates for the polarization modes which are about two orders of magnitude larger than the decay of the optical modes. Accordingly, the optical subsystem (6), (7) also contains two different time-scales with the polarization modes playing no role in the dynamics. The main impact of gain dispersion is the spectral selectivity, shown by the difference between the squares and the crosses in the lower part of Fig.1.

### 3.2 Mode Spectrum of a DFB laser

For a DFB laser, i.e.  $\kappa \neq 0$ , the mode spectrum corresponds to the roots of a complex analytic function resulting from (12). These roots can be obtained for example by numerical continuation starting from the eigenvalues of the Fabry-Perot laser determined by (14). Furthermore, the spectrum of the DFB laser asymptotically approaches the sequence (13) for large  $\omega$  [13]. Hence, only the eigenvalues in the vicinity of the stopband around  $\Re(\beta_k)$  become dominant by introducing some feedback  $\kappa$ .



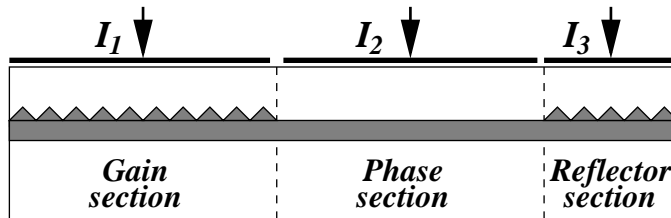


Figure 2: Scheme of a 3-section laser. The outer DFB sections are active, whereas the phase tuning section integrated in the middle is passive.

Our particular example is the three section DFB laser depicted in Fig.2. The device consists of two identical active DFB sections with different lengths and a passive phase tuning section integrated in between. The facets are AR-coated and all sections can be individually pumped. The device parameters are the same as in [11]. Such devices have been used for generating fast self-pulsations (SP) (10-40 GHz)[11] which can be used for example for all-optical clock recovery. In such SP states, to which we focus our interest now, typically one of the DFB sections is pumped well above threshold which we therefore refer to as the “gain” section, whereas the other DFB section is kept at transparency and therefore mainly acts as dispersive “reflector” section. Due to the latter we exclude any carrier dynamics in the reflector section and fix the carriers to transparency for simplicity. The propagation constant  $\beta$  can then be modeled as

$$\beta_3 = \delta_3 - i\alpha_3/2 \quad (16)$$

in the same way as in the passive phase tuning section

$$\beta_2 = \delta_2 - i\alpha_2/2. \quad (17)$$

Consequently the gain in these sections is zero. The contribution from the polarization in these sections has been neglected in our example, by adjusting  $G_r = 0$  there. With respect to the gain this is obvious for the passive phase tuning section, but an assumption for the reflector section. Therefore, in an advanced stage of the model, an explicit carrier dependence of the polarization parameters should be included. The parameters for the polarization in the gain section are given in (15). For carrier densities corresponding to Fig.4(c), the detuning  $\Re(\beta_3) - \Re(\beta_1)$  between the DFB sections nearly vanishes. This is one of the standard situations managed in Self Pulsating 3-section DFB lasers. Furthermore, in a multi-section DFB laser the modes are known to depend on the particular operating state of the device. The SP can be switched on and off very sensitively by tuning the phase conditions (see Fig.4) via the current  $I_2$  [11]. To keep the discussion more intuitive, we express this fine tuning of the operating state via the phase  $\varphi = -\delta_2(I_2) \cdot |L_2|/\pi$ .

To give an example we let  $\varphi = 0$  and discuss the mode spectrum and its correlation to the feedback spectra of the DFB sections, which are shown in Fig.3.

First, we remark that Fig.3 contains only optical modes. The polarization modes still have decay rates two orders of magnitude larger than the optical modes, as in the

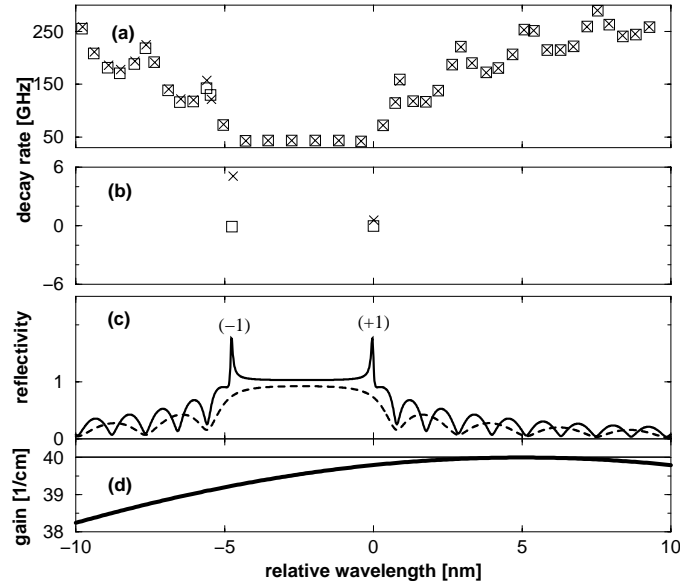


Figure 3: Upper two: Mode spectra of the 3-section DFB laser at the threshold  $N = 1.44 \cdot 10^{18} \text{cm}^{-3}$  with (crosses) and without gain dispersion (boxes). (a): Suppressed modes (b): Dominant modes. Note the different scalings of (a) and (b). (c): reflectivity spectra of the DFB sections. Solid: gain section, dashed: reflector section. The most pronounced modes indicated in (b) are located on the “ears” at the stopband edges of the gain section. Accordingly they are indicated by +1 (long wavelength mode) and -1 (short wavelength mode). (d): material gain dispersion. Thin: standard TWE, thick: extended TWE model.

Fabry-Perot case before. This means that the large gap in the spectrum between the polarization modes and the optical modes in a DFB laser is preserved. Accordingly, we expect the inclusion of polarization to influence the dynamics mainly via the gain dispersion correction of the optical modes. This impact may be significant despite its small magnitude. Typically, as also reflected by the squares in Fig.3(b), the lasing DFB section has two dominant modes spectrally located at the ends of its stopband (c.f. Part (c) of this figure) with almost the same threshold. The frequency of these two modes differs by approximately the stopband width, so the influence of gain dispersion can be strong enough to decide which side of the stopband will be dominant. Fig.3(b) illustrates how the leading modes of a 3-section DFB laser change if we take nonlinear gain dispersion into account. As illustrated in Fig.3(d) and by the crosses in Fig.3(b) gain dispersion prefers the (+1) mode at the long-wavelength end of the stopband in this example. We will see in the next section how this change of the spectral constellation affects the long-time behaviour of the laser.

## 4 Time Domain Simulation of a 3 section DFB laser.

In the following we will compare the solutions of the standard TWE model (1), (2) with the solutions of the extended TWE model (6), (7), (9), varying the primary control parameter  $\varphi$ . This variation of the phase condition in the resonator changes the configuration of the dominant modes (cf. Fig 3.(b)) within the “ears” at the stopband edges of the gain section (cf. Fig 3.(c)). This leads to a complicated bifurcation scenario, including hysteresis and multi-stability. Fig 4.(a) and (b) show the stable stationary and pulsating states, calculated numerically with the standard and the extended TWE model. The calculations are done in the following way: For fixed  $\varphi$  we calculate the transient and record the final state. This state is used as initial state for a calculation with an incremented value of  $\varphi$ .

Typically, when changing the phase  $\varphi$ , jumps between the modes at the (+1) and (-1) edge of the stopband occur. We observe stationary as well as SP states carried by either of such modes, together with a hysteretic switching behaviour. It turns out that this switching behaviour is very sensitive to the material gain margin between the (+1) and (-1) edges of the stopband (cf. Fig 3.). Note that any gain margin, induced by the polarization, is reflected in the difference between the thick and thin carrier density curves in Fig 4.(c). This offset is of course different for (+1) and (-1) modes which may also lead to a change of the location of the mode jumps (cf.  $A$  and  $A'$ ).

Without gain dispersion (Fig 4.(a)), we observe two regions of nearly equal size, where the output is stationary and single moded: Between  $A$  and  $B$  on a (+1) mode, and between  $D$  and  $A$  (i.e. the non hatched region, since  $\varphi$  is periodic) on a (-1) mode. Jumps between stationary states as at  $A$  are typically not hysteretic. At  $B$ , a Hopf bifurcation takes place. Between  $C$  and  $D$ , a large region with hysteretic behaviour appears: For increasing  $\varphi$  a SP state with a dominant (+1) mode can be observed, whereas for decreasing  $\varphi$  the stationary (-1) state extends until it disappears in a saddle-node bifurcation and a (-1) SP state appears. The shaded region between  $B$  and  $C$  with a non hysteretic (+1) SP state is confined to a very small region near the Hopf bifurcation, where the stability of the periodic solution is still weak.

Now, we introduce gain dispersion using the extended TWE model (6), (7), (9). Despite only a small gain margin of about 1/cm, indicated in Fig.3(d), we expect some suppression of the (-1) mode compared to the (+1) mode and hence some stabilization of the laser. Indeed, Figure 4(b) shows some significant changes compared with 4(a): The hatched regions, indicating a dominant (+1) mode become larger, whereas the hysteretic region ( $C', D$ ) is much smaller. Additionally, there now appears a comparatively large region ( $B, C'$ ) with stable, robust and non hysteretic self pulsations. This shows that the relative location of the gain maximum  $\Omega_r$  is an important design parameter for self-pulsating devices and gain dispersion should not be omitted, if an accurate simulation of such effects is required.

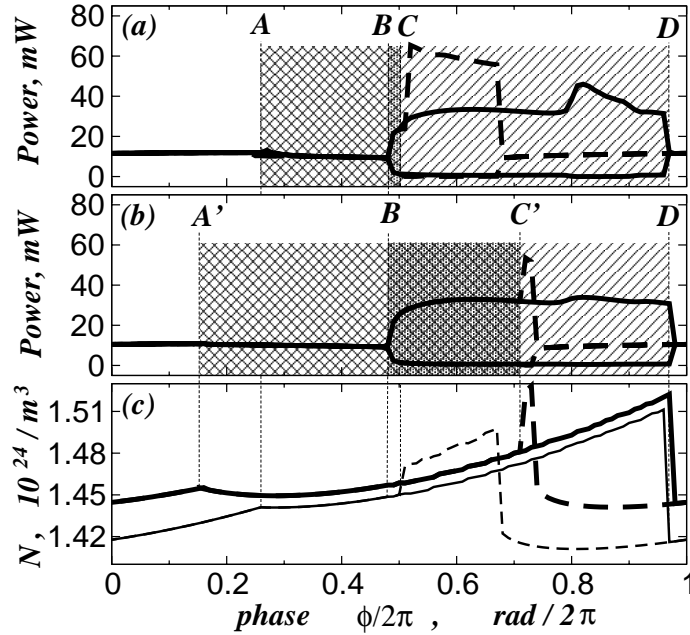


Figure 4: Part (a) and (b): Long time behaviour of the output power in dependence on the phase  $\varphi$  for the TWE- and extended TWE model, respectively. For SP states, maximum and minimum output power at the left facet are plotted. Solid and dashed lines always correspond to increasing resp. decreasing  $\varphi$ . Hysteresis occurs wherever they do not coincide. In hatched regions, the (+1) mode is dominant (simple hatching: only for increasing  $\varphi$ , double hatching: both directions). In the shaded region, a non-hysteretic SP state occurs. Part (c) shows the carrier densities (for SP states averaged) for both models (thick: with gain dispersion).

## 5 Conclusions

In multi-mode semiconductor laser models the inclusion of gain dispersion effects is important and may cause significant changes in the operating states of a device. We have managed this explicitly by applying equations for the polarization with a Lorentzian fit, rather than using filtering techniques or convolution integrals. We obtained an extension of the well known TWE model which is suitable for numerical simulation as well as for analytical investigation of its dynamical properties. From the physical point of view this dispersion is obviously needed for Fabry-Perot lasers but can also be important for DFB lasers. The impact of polarization on mode selectivity can be explained and explicitly calculated using the spectrum of the operator. Our simulations show that under certain conditions remarkable changes in the longtime behaviour of a multi-section DFB laser are caused. Although no new dynamical effects appear from a global point of view, the operating states (e.g. high frequency self pulsations), their stability and dependence on parameters may change substantially. We observed more stable behaviour due to the suppression of side modes by the net gain margin.

## 6 Acknowledgements

We thank H. J. Wünsche (HU Berlin) and H. Wenzel (FBH Berlin) for the many fruitful discussions on laser modeling.

## References

- [1] E.A. Avrutin, J.H. Marsh, J.M. Arnold, "Modelling of semiconductor laser structures for passive harmonic mode locking at terahertz frequencies," *Int. J. of Optoelectr.* vol. 10, n. 6, pp. 427-432, 1995.
- [2] U. Bandelow, H.J. Wünsche, B. Sartorius, M. Möhrle, "Dispersive self Q-switching in DFB-lasers: Theory versus experiment," *IEEE J. Selected Topics in Quantum Electronics*, Vol. 3, pp. 270-278, 1997.
- [3] U. Bandelow, L. Recke, B. Sandstede, "Frequency regions for forced locking of self-pulsating multi-section DFB lasers," *Optics Comm.* 147, pp. 212-218, 1998.
- [4] D. J. Jones, L. M. Zhang, J. E. Carroll, and D. D. Marcenac, "Dynamics of monolytic passively mode-locked semiconductor lasers", *IEEE J. Quantum Electron.*, vol. 31, pp. 1051-58, 1995.
- [5] L. Landau, E. Lifshitz, "Lehrbuch der theoretischen Physik", *Akademie-Verlag Berlin*, Bd. 8, "Elektrodynamik der Kontinua", ch. 9, 1963.
- [6] A. J. Lowery, "New dynamic semiconductor laser model based on the transmission-line modelling method", *IEEE Proceedings: J-Optoelectronics*, vol. 134, n. 5, pp. 281-289, 1987.
- [7] D. Marcenac, "Fundamentals of laser modelling," *PhD thesis, University of Cambridge*, 1993.
- [8] J. Martin-Regalado, S. Balle, N.B. Abraham, "Spatio-Temporal Dynamics of Gain-Guided Semiconductor Laser Arrays," *IEEE J. of Quant. El.*, Vol 32 No. 2, pp. 257-275, 1996.
- [9] C.Z. Ning, R.A. Indik, J.V. Moloney, "Effective Bloch Equations for Semiconductor Lasers and Amplifiers," *IEEE J. of Quant. El.*, Vol 33 No. 9, pp. 1543-1550, 1997.
- [10] B. Sartorius, C. Bornholdt, O. Brox, H.J. Ehrke, D. Hoffmann, R. Ludwig, M. Möhrle "All-Optical Clock Recovery Module Based on a Self-Pulsating DFB Laser," *Electron. Lett.*, 34, pp.1664-1665, 1998.
- [11] M. Radziunas, H.-J. Wünsche, B. Sartorius, O. Brox, D. Hoffmann, K. Schneider and D. Marcenac, "Modeling Self-Pulsating DFB Lasers with Integrated Phase Tuning Section", *to appear in IEEE J. of Quantum Electronics*, 2000.
- [12] J. Rehberg, H.-J. Wünsche, U. Bandelow, H. Wenzel, "Spectral Properties of a System Describing fast Pulsating DFB Lasers," *ZAMM* 77, n.1, pp. 75-77, 1997.

- [13] L. Recke, K.R. Schneider, V.V. Strygin, "Spectral properties of coupled wave equations" *Z. angew. Math. Phys.* 50, pp. 923-933, 1999.
- [14] J. Sieber, U. Bandelow, H. Wenzel, M. Wolfrum, H.-J. Wünsche, "Travelling wave equations for semiconductor lasers with gain dispersion," *WIAS Preprint No.* 459, 1998
- [15] B Tromborg, H.E. Lassen, H. Olesen, "Travelling Wave Analysis of Semiconductor Lasers," *IEEE J. of Quant. El., Vol 30 No. 5*, pp. 939-956, 1994.
- [16] H. Wenzel, U. Bandelow, H.-J. Wünsche, J. Rehberg, "Mechanisms of fast self pulsations in two-section DFB lasers," *IEEE J. Quantum Electron.*, vol. 32, No. 1, pp. 69-79, 1996.